The new cryogenic silicon monolithic micro-bridged AntiCoincidence detector for the X-IFU of ATHENA

M. Biasotti*[a], D. Corsini [a], M. De Gerone[a], F. Gatti[a], C. Macculi[b], M. D'Andrea[b], L. Piro[b].
[a]Università di Genova, & INFN sez. di Genova, via Dodecaneso 33 16146 Genova Italy
[b]INAF-IAPS Roma, Via del Fosso del Cavaliere, 100, 00133 Roma, Italy

ABSTRACT

The new monolithic micro-bridged Cryogenic Anticoincidence for the X-IFU instrument of ATHENA has been designed. It is a single pixel made of silicon with Ir-Au TES array that respond to all the requirements of the recently closed design review phase. It is the natural prosecutor of the previous version without micromachined bridges (pre-demonstration model) It has shape has been fully characterized and its data were used to improve the new design. In this paper, we report the overview of this work of fabrication test and design. A preliminary delivery test with 60 keV gamma ray is also described.

Keywords: ATHENA, CryoAC, TES

1. INTRODUCTION

The ATHENA (Advanced Telescope for High ENergy Astrophysics)[1] satellite will have two focal plane instruments, the X-IFU [2] and the WFI[3]. Those instruments are complementary each other: the first one will provide images over a small FoV (5' arcminute) and very high spectral energy resolution, 2.5 eV FWHM in the energy range 0.2-12 keV, featuring for the first time the "Integral field spectroscopy", whereas the second will provide image over a wide FoV (40'x40') but featured by low energy resolution (< 150eV@6keV).

Among the X-IFU scientific goals the high spectral energy resolution map of faint or diffuse sources are very important. Hence the background events from the cosmic particle on the TES-microcalorimeter array can submerge the X-ray signals. It is necessary to reduce the background events at the L2 orbit by a factor around 10^3 down to the goal of 0.005 cts/cm^2/s/kev [4]. This operation will done by an active Cryogenic AntiConcidence detector (CryoAC), and a passive secondary electron shielding surrounding the TES-array.

The CryoAC baseline design is based on a thin (0.5 mm) Si absorber where the energy deposited by the cosmic particles is sensed by an array of small Ir TES deposited on its surface. The detector is located 0.5 mm beneath the X-IFU TES microcalorimeter array and has a total active area of 4.6 cm^2 on 4 pixels, each of ~ 1.15 cm^2. The 4 pixels are conceived in order to respond to the requirement of greater redundancy, lower dead time, and easier achievement of energy dynamic range from 20 keV to 0.5MeV.
In this paper are shown the progresses in the design, development, and test of the CryoAC: in section 2 we describe the pre-demonstration model (pre-DM), in section 3 we report its characterization including test with 60 keV gamma ray for simulating GeV protons, and in section 4 a description of demonstration model (DM) design is reported.

*Michele.biasotti@ge.infn.it

Space Telescopes and Instrumentation 2016: Ultraviolet to Gamma Ray, edited by
Jan-Willem A. den Herder, Tadayuki Takahashi, Marshall Bautz, Proc. of SPIE Vol. 9905, 99055Z
· © 2016 SPIE · CCC code: 0277-786X/16/$18 · doi: 10.1117/12.2232789

2. PRE-DEMONSTRATION MODEL DESCRIPTION

The design and fabrication of the DM needs the full understanding of the main physics processes ruling the detector dynamic. It has been clear since the beginning that the A-thermal signal produced in the primary events of proton interaction with the silicon absorber was an important contribution for achieving fast pulse rise-time in so large absorber. Due to the anisotropy or the emission of such A-thermal phonons[5, 6], several different prototypes were developed in order to understand how to collect efficiently them[7]. The last prototype, AC-S7 prototype also named "Pre-DM", has reached the expected performance. It was produced from a silicon wafer at the Genova University (Phys. Dept.), the sensing structure is made of 65 TESs uniformly distributed on one silicon face, each with 100 × 100 μm^2 area and 200-nm-thick Ir film, that has been grown with Pulsed Laser Deposition. The TESs are parallel connected, through niobium striplines deposited with RF sputtering (see table 1). The thermal conductance is made by using a second silicon wafer as heat sink: the "active detector" is linked to the sink with 4 SU-8 hollow towers filled with epoxy glue. Those towers connect the backside of detector active chip to the thermal sink that is in strong thermal contact to the bath. The shape of towers allows us to control the thermal conductance, which is expected to be 10^{-8} W/K. In figure 1 is reported this description and a picture of the device, in particular figure 1a shows the tower mechanism to perform the thermal link.

Table 1. AC-S7 "pre-DM" constructive properties.

AC-S7 "Pre-DM" FABRICATION PARAMETERS	
Parameter	Value
Absorber Silicon Area	10 x 10 mm^2
Absorber Silicon Thickness	380 µm
TES (x65) Iridium Area	100 x 100 μm^2
TES (x65) Iridium Thickness	200 nm
R_N	1.5 mΩ
Epoxy Tower	500 x500 x50 μm^3

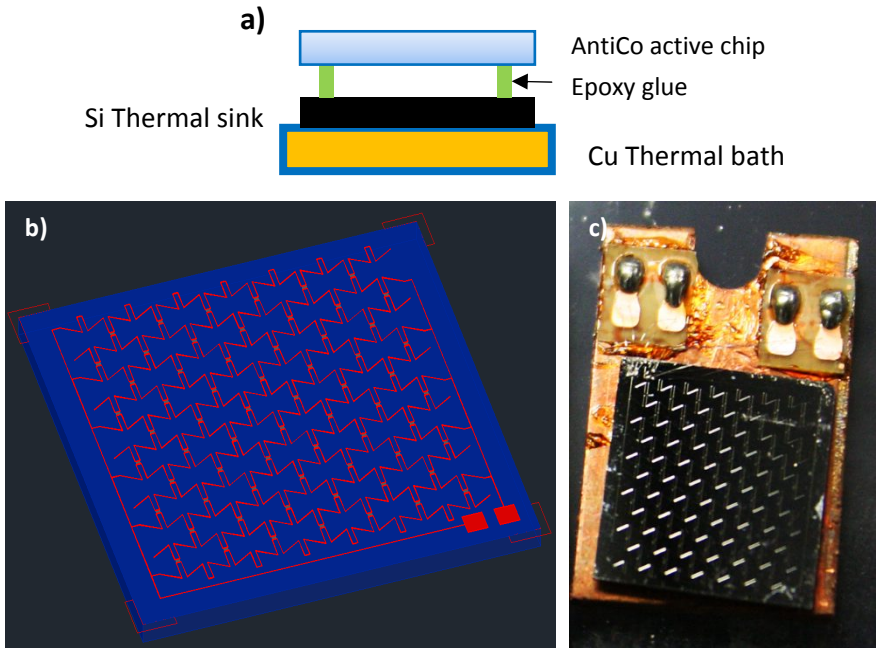

Figure 1. AC-S7 "Pre-DM": a) scheme of "tower" thermal connection; b) rendering of active chip; c) picture of the device mounted on copper support.

3. PRE DEMONSTRATION MODEL CHARACTERIZATION

The AC-S7 pre-DM detector initially was characterized by standard measurements: transition curve (resistance vs. temperature) and load curves (current vs. voltage), without any radiation source. Transition curve was performed both using four probes techniques with constant current bias and using a SQuID to read the current at constant voltage bias (see fig. 2). Load curves were performed scanning bias condition with a slow voltage ramp. The current going through TES was measured with commercial SUPRACON SQuID system. Figure 3 reports several load curves at different temperatures, an instability was observed at low temperature and low bias. Fitting load curves in neighborhood of the zero bias it is possible to extrapolate the zero-bias power TES resistance (see inset fig 3). The pre-DM has shown a normal resistance R_0 = 1.5 mΩ. This so low resistance is due to the parallel connection of 65 identical iridium TES (each TES has a normal resistance of about 100 mΩ). Their Transition temperature is 124 mK and we highlight a good uniformity as shown by the total transition width (10%-90%) of only 2.4 mK. These data imply an alpha value up over 100 at 122 mK, and a thermal conductance of $2 \cdot 10^{-8}$ W/K. A so strong thermal coupling produce the necessity of large bias current to drive TESs in transition region. In the curves at lowest temperature, it was observed an instability probably due to the strong electro-thermal feedback.

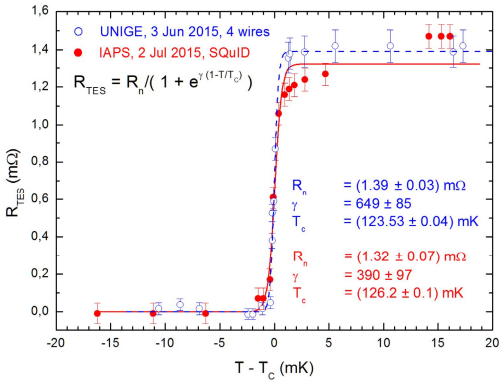

Figure 2. Transition curve measured with constant bias at university of Genoa (UNIGE) with four probes technique and at IAPS using SQuID setup.

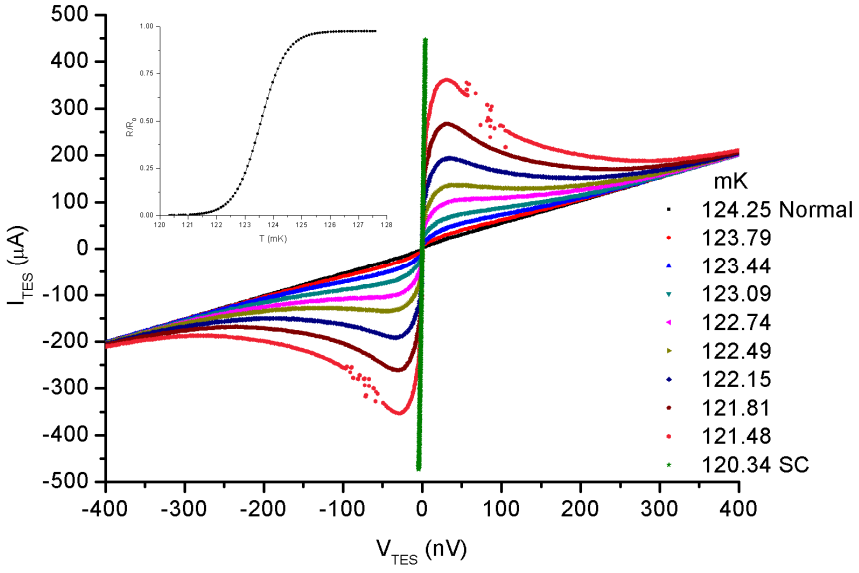

Figure 3. Load curves at different temperature. Inset: R(T) plot by load curve fitting. Only a subset of load curves has been plotted for clarity.

3.1 Pulse detections of 60 keV gamma from ^{241}Am

We have used an ^{241}Am calibration source to simulate the energy left by a GeV charged particle in operating conditions. At first attempt we used commercial SUPRACON SQuID setup but its relatively large input inductance reduced the bandwith. Therefore we changed the readout setup and used the J3-model VTT SQuIDs with Magnicon C6X216FB electronics. In figure 4 are reported two pulses detected with both readout electronis. The first one (left) with commercial SURACON system and the second one (right) with VTTSQuID-MAGNICON system. In the former, the A-thermal signal is stretched: this effect is due to bandwith limitations caused by the large SQuID input inductance. In the latter, this deformation is limited. In figure 5 is reported the spectrum obtained from pulses analysis (for more detail concerning the pulse analysis see M. D'Andrea et al.[8]in these procedeengs). The 60 keV peak is clearly visible and the threshold of 20 keV is well detectable.

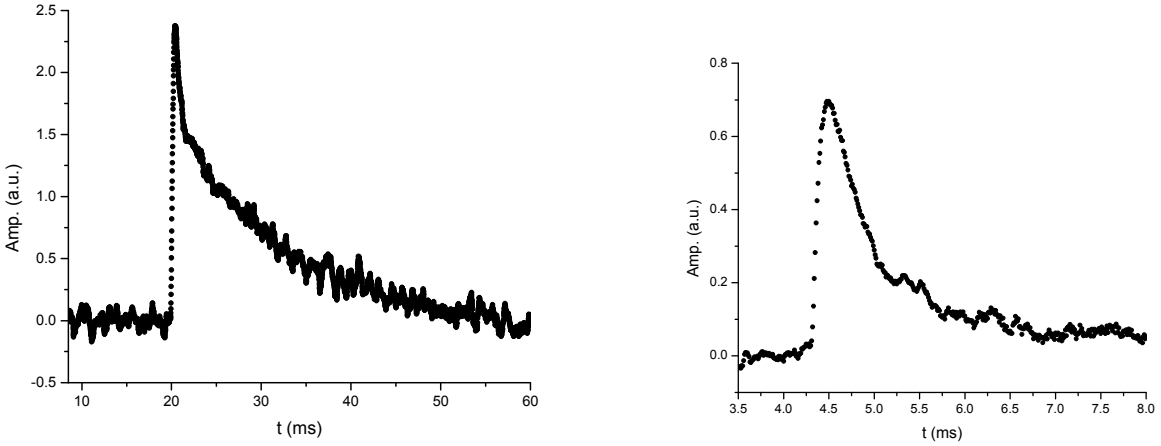

Figure 4. pulses detected with supracon SQuID (left) and VTT SQuID (right). The Athermal pulse in the "Supracon" pulse (left) is starched.

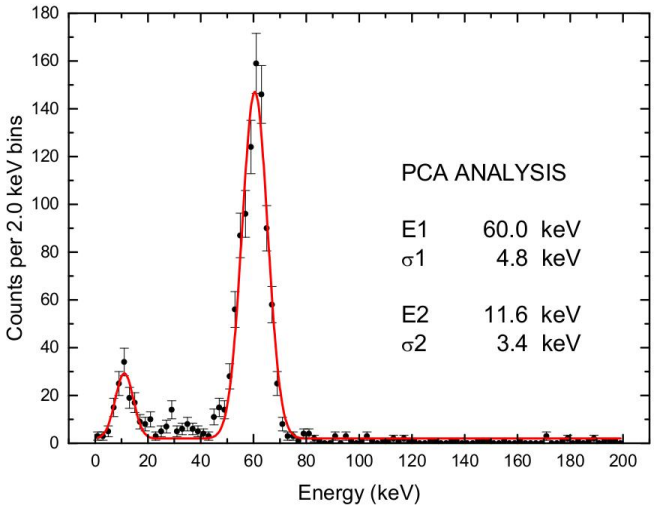

Figure 5. Energy spectrum observed on AC-S7 "Pre-DM" illuminated with Am^{241} gamma source. (see M. D'Andrea et al. paper [8])

4. DEMONSTRATION MODEL DESIGN

The next step is the production and test of the "demonstration model" (DM). It represents a prototype in which the main critical aspects are solved. The main issue is the control of thermal conductivity; in particular, in place of the epossidic towers the DM will be made of "suspended" silicon absorber using planar silicon bridges in order to have a well reproducible thermal conductance, smaller size and higher mechanical stability. Moreover, it will operate at 50 mK of thermal bath temperature. The path towards the final realization of the CryoAC DM (Figure 6, Left) envisages the development and measurement of Silicon test structure of bridges prototypes with the aim to determine silicon thermal conductivity. (Figure 6, Right). Since the aim of DM is to increase the detector "maturity" and it has not to be fully representative of the flight model, it will be developed matching as much as possible the requirements and specifications (see C. Macculi et al. paper[9]).

The CryoAC DM is a single pixel freestanding detector covered by 96 rectangular TESs laying on the Silicon chip, carved out from a 16.8x16.8 squared mm of double side polished silicon wafer and suspended by 4 bridges, 100 µm wide and 1000 µm long (see table 2). The TESs configuration and distribution on the silicon active area (i.e., the absorber) is driven by two requirements: to minimize the Ir-Au volume, (to not increase thermal capacity of the CryoAC) and to uniform as much as possible the response to the A-thermal component of the primary signal generated by energy deposition of energetic particles. The development is ongoing.

Table 2. DM actual design.

DM CONSTRUCTIVE PARAMETERS	
Parameter	Value
Chip Area	16.8 x 16.8 mm^2
Chip Thickness	500 µm
TES number	96
Bridge number	4
Bridge length	1000 µm
Bridge width	100 µm

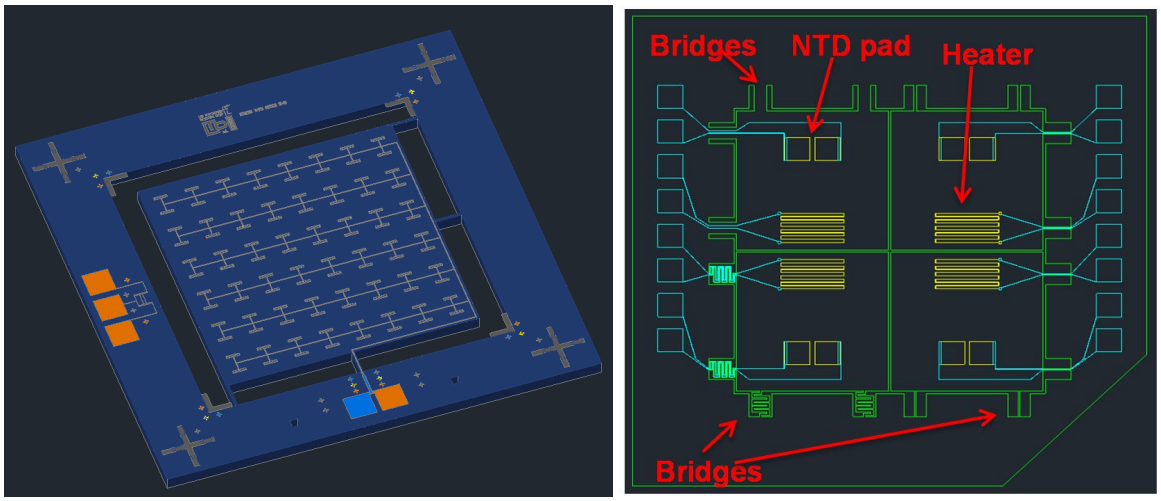

Figure 6. Left – The CryoAC DM. Right - Test structure mask: 4 different configuration of the Silicon beams.

5. CONCLUSION

In conclusion, the AC-S7 "pre-DM" has shown the suitability of this technology for development of anticoincidence device. The development of DM, having a monolithic detector, which will solve the last issues, is ongoing.

ACKNOWLEDGEMENT

This work has been partially supported by ASI (Italian Space Agency) through the Contract no. 2015-046-R.0

REFERENCES

[1] Nandra, K., Barret, D., Barcons, X., Fabian, A., den Herder, J.-W., Piro, L., Watson, M., Adami, C., Aird, J., Afonso, J. M., and et al., "The Hot and Energetic Universe: A White Paper presenting the science theme motivating the Athena+ mission," 2013arXiv1306.2307N (2013).

[2] Barret, D., den Herder, Jan-Willem, Piro, L., T. L. Trong, X. Barcons, "The ATHENA X-ray Integral Field Unit", in this proceeding, paper 9905-83 (2016).

[3] Rau, A., Meidinger, N., Nandra, K., et al, "The Hot and Energetic Universe: The Wide Field Imager (WFI) for Athena+", 2013arXiv1308.6785, (2013).

[4] C. Macculi et al., "The Cryogenic AntiCoincidence Detector for the ATHENA X-IFU: Design Aspects by Geant4 Simulation and Preliminary Characterization of the New Single Pixel" J. Low Temp. Phys. (2016)

[5] Macculi C. et al., "The Cryogenic AntiCoincidence detector for ATHENA: the progress towards the final pixel design", Proc. of SPIE Vol. 9144, 91445S, (2014).

[6] Macculi C. et al., "The Cryogenic AntiCoincidence detector for the ATHENA X-IFU: design aspects by Geant4 simulation, and preliminary characterization of the new single pixel", J. Low Temp. Phys. 184, pp. 680-687 DOI 10.1007/s10909-015-1439-y, (2016).

[7] C. Macculi, L. Piro, L. Colasanti, S. Lotti, L. Natalucci, D. Bagliani, M. Biasotti, F. Gatti, G. Torrioli, M. Barbera, T. Mineo, E. Perinati, "The Cryogenic AntiCoincidence Detector Project for ATHENA+: An Overview Up to the Present Status" J. Low Temp. Phys., 176, pp. 1022-1032 DOI 10.1007/s10909-014-1150-4 (2014)

[8] D'Andrea M. et al., "The Cryogenic Anti-Coincidence detector for ATHENA X-IFU: pulse analysis of the AC-S7 single pixel prototype", in this issue, paper 9905-185 (2016).

[9] Macculi C. et al, "The Cryogenic AntiCoincidence Detector for ATHENA X-IFU: a program overview", in this issue, paper 9905-88 (2016).